

IOWA STATE UNIVERSITY

AIRFOIL WAKE MEASUREMENTS AND
CALIBRATION OF A HOT WIRE ANEMOMETER
LABORATORY

AER E 344 - LAB 06 - AIRFOIL WAKE MEASUREMENTS AND
CALIBRATION OF A HOT WIRE ANEMOMETER

SECTION 3 GROUP 3

MATTHEW MEHRTENS
JACK MENDOZA
KYLE OSTENDORF
GABRIEL PEDERSON
LUCAS TAVARES VASCONCELLOS
DREW TAYLOR

PROFESSOR

HUI HU, PhD

College of Engineering
Aerospace Engineering
Aerodynamics and Propulsion Laboratory

AMES, MARCH 2024

ABSTRACT

Using the low-speed wind tunnel at Iowa State University, we analyzed the wake distribution of an airfoil using a pressure rake connected to pressure transducers. We collected pressure data from the pressure rake for different angles of attack to create a profile of the airfoil wake region and estimate the coefficient of drag. Our data showed the presence of significant turbulence and vortices at angles of attack greater than 12° . Additionally, to facilitate more precise velocity measurements in future labs, we calculated the fourth order calibration curve of a hot wire anemometer to relate the measured voltage to airspeed.

CONTENTS

Contents	ii
List of Figures	iii
List of Tables	iv
Glossary	v
Acronyms	1
1 Introduction	2
2 Methodology	3
2.1 Apparatus	3
2.1.1 Airfoil Wake Measurements	3
2.1.2 Hot Wire Anemometer Calibration	3
2.2 Procedure	4
2.2.1 Airfoil Wake Measurements	4
2.2.2 Hot Wire Anemometer Calibration	4
2.3 Derivations	5
3 Results	7
4 Discussion	10
5 Conclusion	11
A Appendix A	13
A.1 Additional Figures	13
B Appendix B	20
B.1 Data	20
C Appendix C	23
C.1 Lab6Analysis.m	23
C.2 Lab6HotWire.m	25

LIST OF FIGURES

2.1	Image of Airfoil and The Pressure Rake in Test Section.	3
2.2	Image of the small open Circuit wind tunnel.	4
2.3	Image of the Hot Wire Anemometer inside of open Circuit wind tunnel.	5
3.1	Plot of the Consolidated Pressure distributions.	7
3.2	Plot of the C_d in relationship to the AoA.	8
3.3	Plot of the Velocity of the air vs the voltage of the Hot Wire Anemometer	8
A.1	plot of the coefficient of pressure vs the angle of attack at zero degrees.	13
A.2	plot of the coefficient of pressure vs the angle of attack at four degrees.	14
A.3	plot of the coefficient of pressure vs the angle of attack at six degrees.	14
A.4	plot of the coefficient of pressure vs the angle of attack at eight degrees.	15
A.5	plot of the coefficient of pressure vs the angle of attack at 10 degrees.	15
A.6	plot of the coefficient of pressure vs the angle of attack at Twelve degrees.	16
A.7	plot of the coefficient of pressure vs the angle of attack at fourteen degrees.	16
A.8	plot of the coefficient of pressure vs the angle of attack at sixteen degrees.	17
A.9	Plot of the magnitude of the coefficient of drag versus the angle of attack of an airfoil.	17
A.10	Image of the Hot Wire data collection computer.	18
A.11	Open loop wind tunnel speed controller and the Mensor manometer	18
A.12	Image of the Hot Wire Anemometer inside of open Circuit wind tunnel.	19

LIST OF TABLES

B.1	Coefficient of Pressure, C_P , at taps 1-23 on the pressure rake at different angles of attack.	20
B.2	Coefficient of Pressure, C_P , at taps 24-46 on the pressure rake at different angles of attack.	21
B.3	C_d at different airfoil angles of attack.	21
B.4	Manometer pressure, anemometer voltage, and flow velocity values at different percents of wind tunnel motor maximum frequency.	22

GLOSSARY

C	Chord length. (p. 6)
C_P	Dimensionless coefficient of pressure. (p. iv, 10, 11, 13–17, 20, 21)
C_d	Dimensionless coefficient of drag. (p. iii, iv, 7, 8, 10, 11, 17, 21)
K	Wind tunnel calibration constant. (p. 5)
P_A	Static pressure at the inlet of the contraction section. (p. 5)
P_E	Static pressure at the entrance of the test section. (p. 5)
V	Voltage. (p. 7)
d	Distance between pressure taps in the pressure rake. (p. 6)
q_∞	Free stream dynamic pressure. (p. 5)
v	Velocity or air speed. (p. 7)
y	The vertical position downstream of the airfoil. (p. 6)

ACRONYMS

AoA angle of attack. (*p.* *iii, 4, 7, 8, 10, 11, 13–17*)

MATLAB MATrix LABoratory. (*p.* *10*)

INTRODUCTION

The Scanivalve DSA 3217, a 16-channel digital pressure transducer, calculates the differences in pressure between the input ports and the calibrated reference pressure. In this experiment, the ports of the pressure transducer are connected to pressure taps on a pressure rake located downstream of an airfoil in the test section of a wind tunnel (see [Figure 2.1](#)). Also in this experiment, a hot-wire anemometer is placed in a small wind tunnel for calibration using a pitot-tube connected to a Mensor manometer.

Using pressure measurements from the Scanivalve pressure transducers in conjunction with the data acquisition software, we will measure the pressure due to an airfoil's wake on a pressure rake (see [Section B.1](#)). After post-processing using the script in [Section C.1](#), a view of the wake region will be shown (see [Chapter 3](#)). The drag coefficients will also be determined from this data and compared to the calculations done for Lab 5 in [Chapter 4](#).

METHODOLOGY

2.1 Apparatus

2.1.1 Airfoil Wake Measurements

An airfoil is positioned in the wind tunnel test chamber as seen in [Figure 2.1](#). Downstream of the airfoil is a pressure rake consisting of 46 pressure taps, each spaced 2 mm apart. The pressure taps are connected to Scanivalve pressure transducers. A computer with data acquisition software collects measurements from the pressure transducers and stores the data in .csv files.

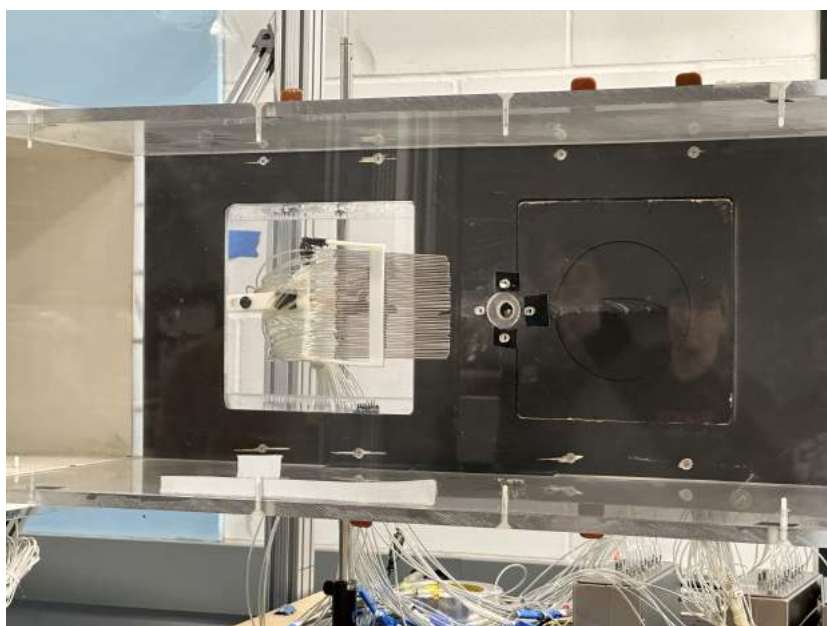


Figure 2.1: Photograph of the airfoil and the pressure rake in the test section of the wind tunnel.

2.1.2 Hot Wire Anemometer Calibration

A hot wire anemometer and pitot tube are positioned in the test chamber of a small wind tunnel as seen in [Figure 2.2](#) and [Figure 2.3](#). The pitot tube is connected to a Mensor

manometer. Both the anemometer and Mensor manometer are connected to a computer with data acquisition software to collect measurements and store the data in .txt files.

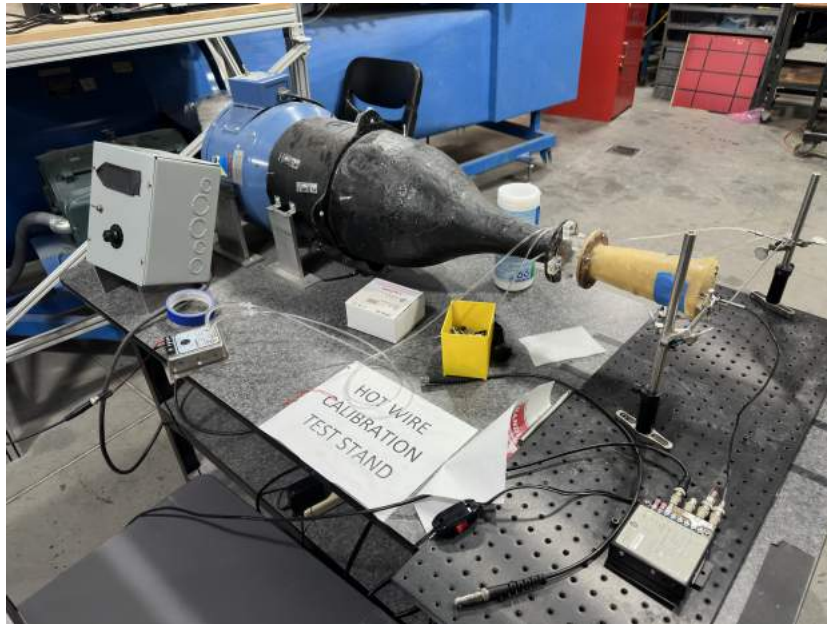


Figure 2.2: Photograph of the open-loop hot wire calibration wind tunnel.

2.2 Procedure

2.2.1 Airfoil Wake Measurements

1. Calibrate the instruments with the wind tunnel set to 0 Hz.
2. Set the wind tunnel velocity at 15 Hz. Wait for velocity to become relatively uniform.
3. Set the AoA to 0° .
4. Move the rake to cover the entire wake of the airfoil as necessary.
5. Acquire and save the data to a data file.
6. Repeat steps 3-4 using the following AoAs: 4, 6, 8, 10, 12, 14 and 16.
7. Save the data to a flash drive for past-lab analysis.

2.2.2 Hot Wire Anemometer Calibration

1. Set the hot wire calibration tunnel to 20 % power.
2. Record the voltage data acquired by the data acquisition software and the pressure data from the Mensor digital pressure gauge.
3. Repeat steps 1-2 for 20 % to 60 % power in increments of 4 %.
4. Save the data to a flash drive for post-lab analysis.

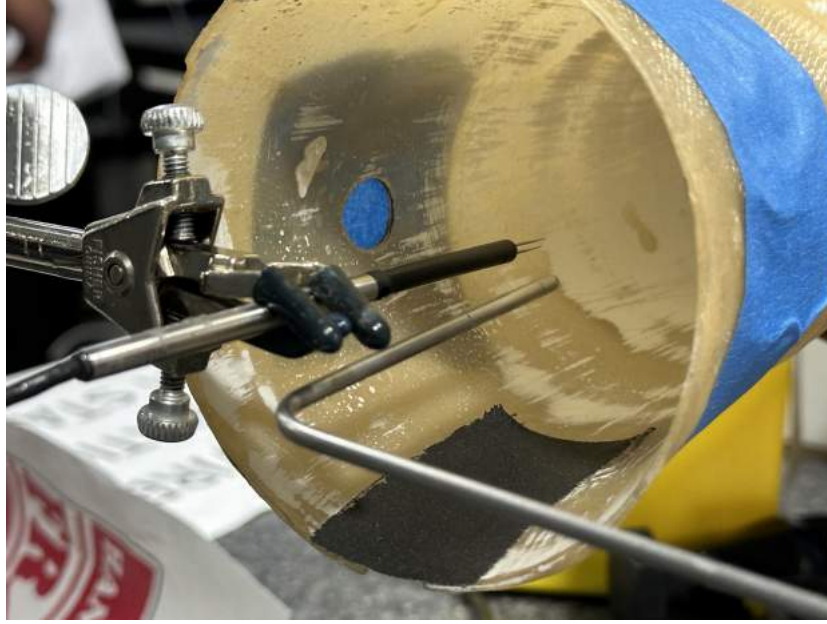


Figure 2.3: A close-up photograph of the hot wire anemometer and pitot tube in the hot wire calibration wind tunnel.

2.3 Derivations

The coefficient of pressure is found by normalizing the dynamic pressure measured by the pressure taps with the free-stream dynamic pressure. The difference between the inlet and outlet pressure of the contraction section, P_A and P_E , respectively, along with the wind tunnel calibration constant, K , determines the free-stream dynamic pressure denoted by q_∞ .

$$q_\infty = K(P_A - P_E) \quad (2.1)$$

The dynamic pressure at a singular tap from the pressure rake, generically described as the i th tap, is found by subtracting the total pressure measured by the tap with the free-stream static pressure.

$$q_i = P_i - P_E \quad (2.2)$$

Therefore, the coefficient of pressure can be found by dividing Equation 2.2 by Equation 2.1:

$$C_P = \frac{q_i}{q_\infty} = \frac{P_i - P_E}{K(P_A - P_E)} \quad (2.3)$$

To begin calculations on the coefficient of drag, the flow velocity at each pressure tap is found by rearranging the generic dynamic pressure equation, $q = \frac{1}{2}\rho V^2$.

$$U_i = \sqrt{\frac{2q_i}{\rho}} = \sqrt{\frac{2(P_i - P_E)}{\rho}} \quad (2.4)$$

The free-stream flow velocity is found similarly:

$$U_\infty = \sqrt{\frac{2q_\infty}{\rho}} = \sqrt{\frac{2K(P_A - P_E)}{\rho}} \quad (2.5)$$

The coefficient of drag is found by using the fluid momentum change as drag resulting in Equation 2.6, where C is the chord of the airfoil and y is the area downstream of the airfoil (Hu, 2024).

$$C_D = \frac{2}{C} \int \left[\frac{U_y}{U_\infty} \left(1 - \frac{U_y}{U_\infty} \right) \right] dy \quad (2.6)$$

The coefficient of drag can be approximated with the data collected from the pressure rake using a Midpoint Riemann Sum of the pressure taps, where C is the chord and d is the distance between each pressure tap.

$$C_D = \frac{2}{C} \sum_{i=1}^{45} d \frac{\left[\frac{U_i}{U_\infty} \left(1 - \frac{U_i}{U_\infty} \right) \right] + \left[\frac{U_{i+1}}{U_\infty} \left(1 - \frac{U_{i+1}}{U_\infty} \right) \right]}{2} \quad (2.7)$$

RESULTS

Figure 3.1 shows pressure distributions at various AoA. Section A.1 has graphs for each of the pressure coefficient distributions.

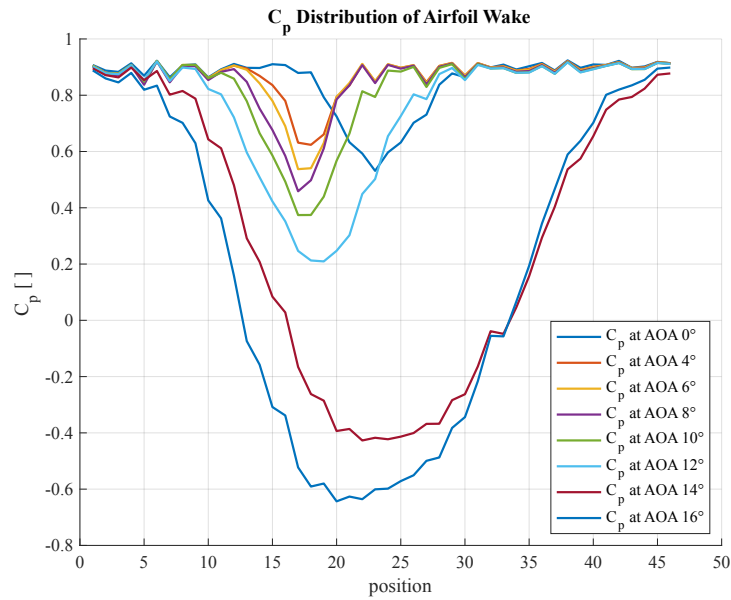


Figure 3.1: Plot of the pressure coefficient distributions overlaid.

Figure 3.2 shows the estimated Coefficient of Drag, C_d , over the 0° to 16° AoA we measured with the pressure rake. Figure 3.3 shows the hot wire calibration curve we calculated based on our calibration data. The fourth order polynomial we calculated is shown in Equation 3.1

$$v = -4982.7570V^4 + 24021.8937V^3 + -43230.9413V^2 + 34446.6867V + -10248.1714 \quad (3.1)$$

where v is the air speed and V is the voltage of the hot wire anemometer.

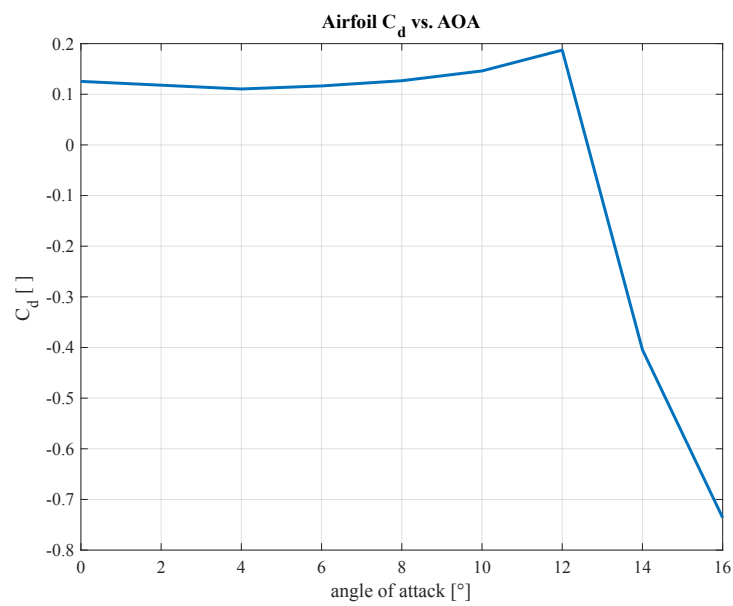


Figure 3.2: Plot of the C_d in relationship to the AoA.

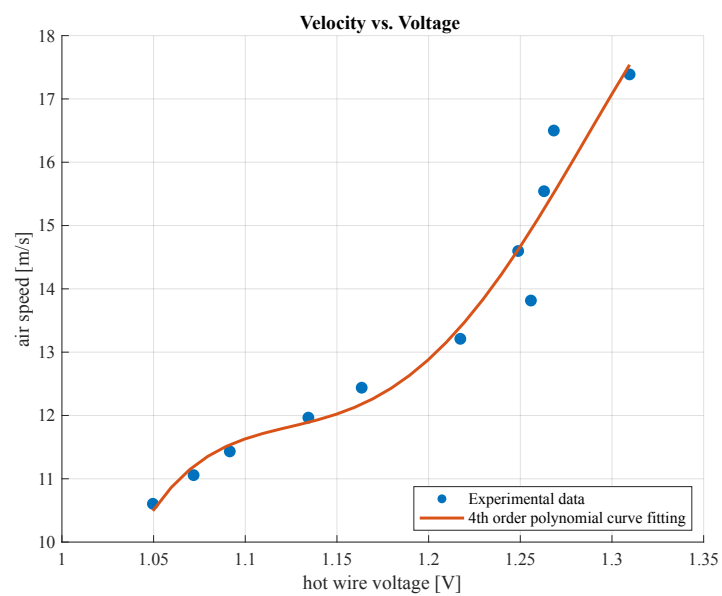


Figure 3.3: Plot of the air speed vs. the voltage reading from the hot wire anemometer.

Using Equation 3.2 and the subsequent parameters, we find the Reynolds number of about 1.1×10^5 for the airfoil wake measurements.

$$Re = \frac{\rho VL}{\mu} \quad (3.2)$$

$$\rho = 1.225 \text{ kg/m}^3$$

$$\mu = 18.18 \times 10^{-6} \text{ Pa s}$$

$$L = 0.101 \text{ m}$$

$$V = 16.1 \text{ m/s}$$

$$Re = 1.09569 \times 10^5$$

DISCUSSION

All of the C_p distribution graphs are shown in [Section A.1](#) but [Figure 3.1](#) is more demonstrative. From [Figure 3.1](#), we note that as the angle of attack increases, the wake region becomes wider and more turbulent. Once the AoA reaches 14° , the C_p in the wake becomes negative—denoting the presence of vortices and turbulence that are causing the flow to reverse direction. This aligns with the visual demonstrations we observed in the smoke tunnel during the first lab where significant vortices formed in the wake region of the airfoil as the angle of attack increased.

Using our MATrix LABoratory (MATLAB) script (see [Section C.1](#)) and the equations derived in [Section 2.3](#), we calculated and plotted the coefficient of drag, C_d , against the angle of attack as shown in [Figure 3.2](#). For AoA 0° to 12° , the C_d plot generally matches what we would expect from a coefficient of drag graph. For 14° and 16° , however, the C_d turns negative. Although unorthodox, this reaffirms the observations made in the 14° and 16° C_p plots: at very high angles of attack, turbulent vortices are causing the flow in the wake to move in the opposite direction of the free stream flow. If only the magnitude of the drag coefficient is considered (see [Figure A.9](#)), the shape of the C_d graph matches what we would expect from an airfoil undergoing low-speed flow.

Although the magnitudes of the drag coefficients in our data vary slightly from the magnitudes of the drag coefficients in lab five, the shape is almost identical—especially when compared to [Figure A.9](#). In both lab five and this lab, the lowest magnitude of the coefficient of drag occurs at 4° to 6° with a clearly defined stall occurring just after 12° .

The fourth order polynomial, [Equation 3.1](#), we calculated for the hot wire calibration curve (see [Figure 3.3](#)) using the script in [Section C.2](#) seems to fit well visually. The coefficient of determination was calculated to be 0.95 which shows high correlation. With the data we collected, a third order polynomial may also have fit well, but if we had additional data points between 16.5 m/s and 17.5 m/s, a third order polynomial may have been inadequate.

CONCLUSION

Using the Scanivalve DSA 3217 pressure transducers, we measured pressure from 46 taps on the pressure rake downstream of an airfoil in the wind tunnel for a range of angle of attacks at a constant fluid velocity. The C_P graphs show as angle of attack increases, the wake region increases, resulting in decreasing values of C_P as you move towards the central taps of the pressure rake. The wake region is much larger at AoA larger than the stall angle of 12° as seen in [Figure 3.1](#) due to flow separation and turbulence. The C_d graph is similar to that of lab five as it shows the stall angle and has around the same AoA for the minimum C_d at angles of attack less than the stall angle. However, the magnitude of C_d differs and the behavior of C_d differs at AoA greater than the stall angle.

BIBLIOGRAPHY

Hu, Hui (2024). *Airfoil Wake Measurements and Calibration of a Hot Wire Anemometer*. Iowa State University. URL: https://www.aere.iastate.edu/~huhui/teaching/2024-01S/AerE344/lab-instruction/AerE344L-Lab-06-instruction_Wake-Hotwire-caliboration-2024.pdf.

APPENDIX A

A.1 Additional Figures

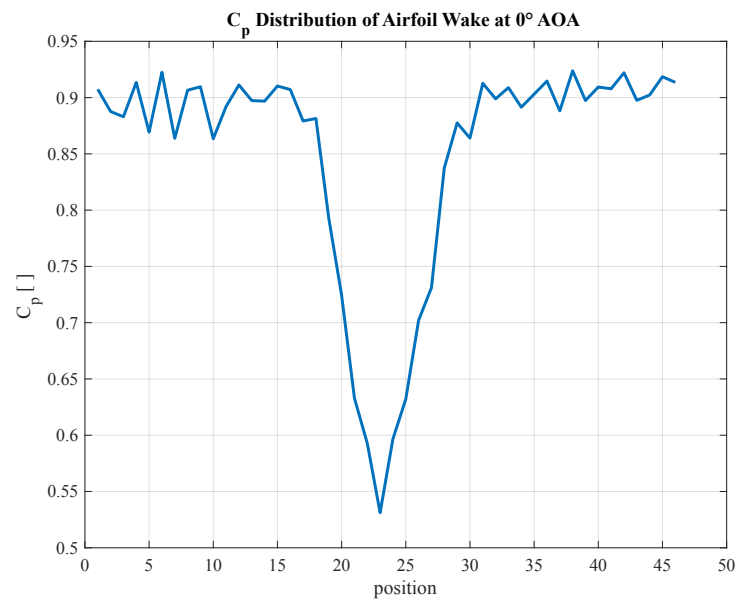


Figure A.1: Plot of C_p distribution vs the Airfoils wake at an AoA of 0°

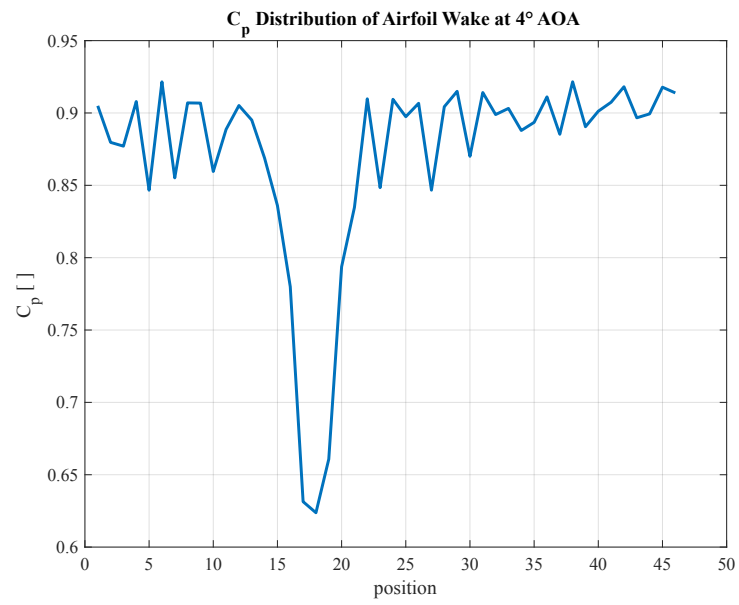


Figure A.2: Plot of C_p distribution vs the Airfoils wake at an AoA of 4°

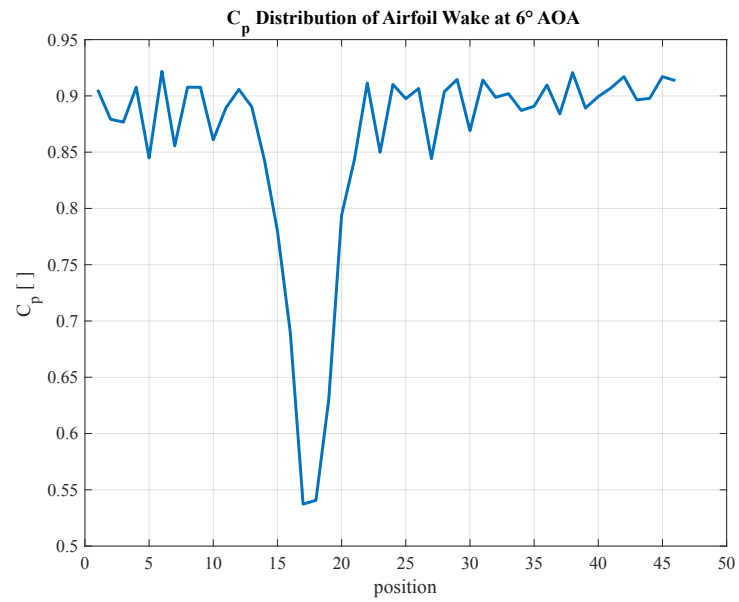


Figure A.3: Plot of C_p distribution vs the Airfoils wake at an AoA of 6°

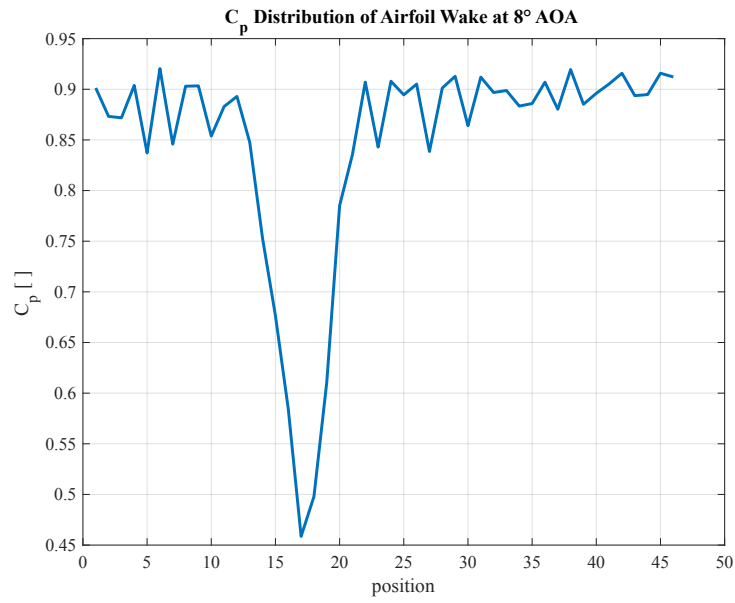


Figure A.4: Plot of C_p distribution vs the Airfoils wake at an AoA of 8°

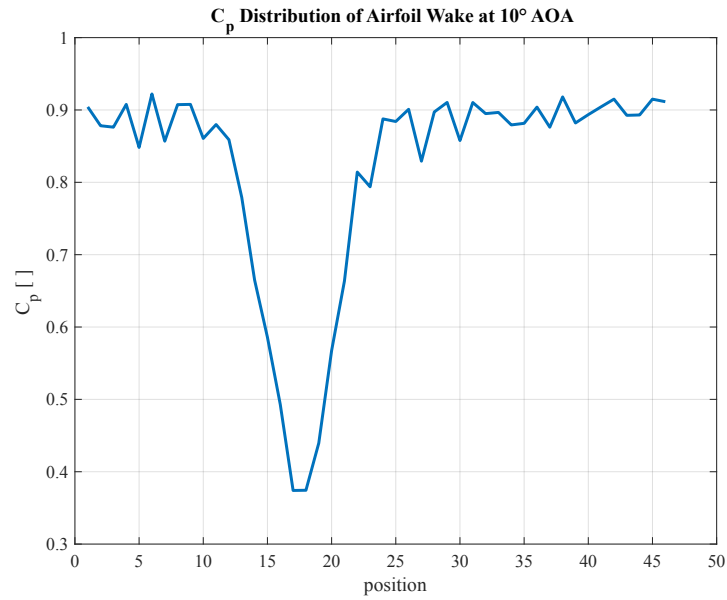


Figure A.5: Plot of C_p distribution vs the Airfoils wake at an AoA of 10°

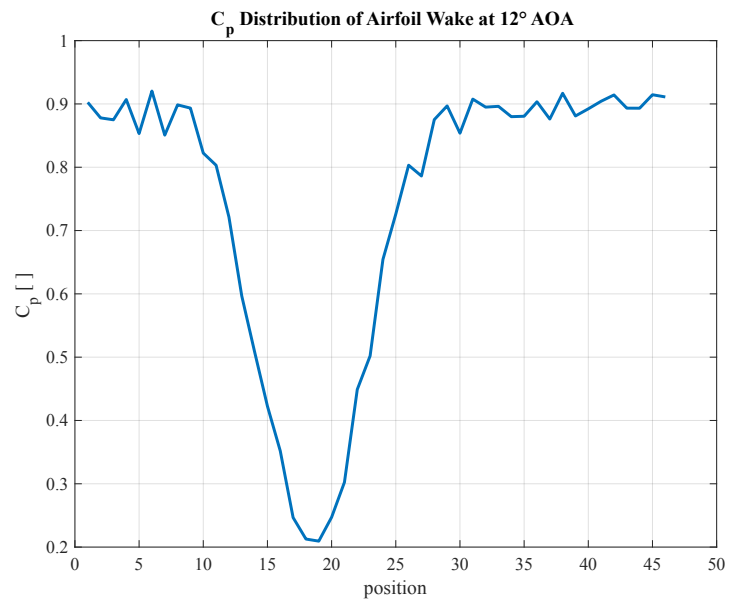


Figure A.6: Plot of C_p distribution vs the Airfoils wake at an AoA of 12°

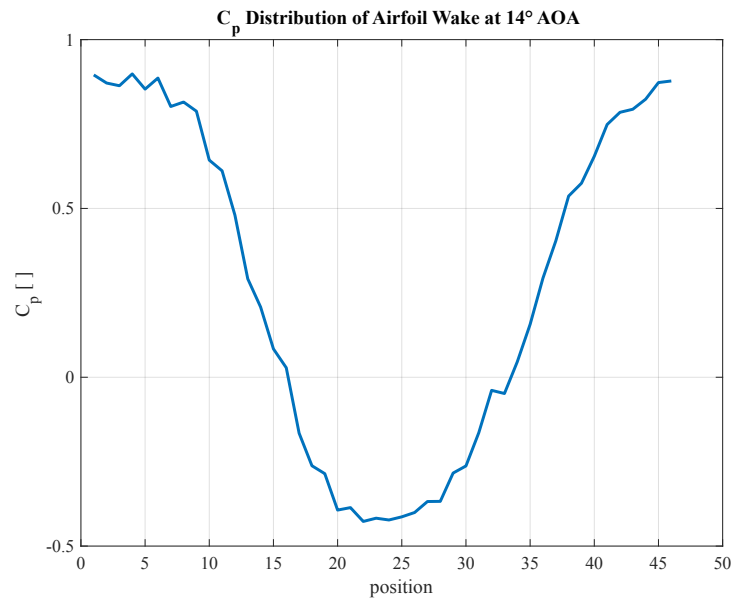


Figure A.7: Plot of C_p distribution vs the Airfoils wake at an AoA of 14°

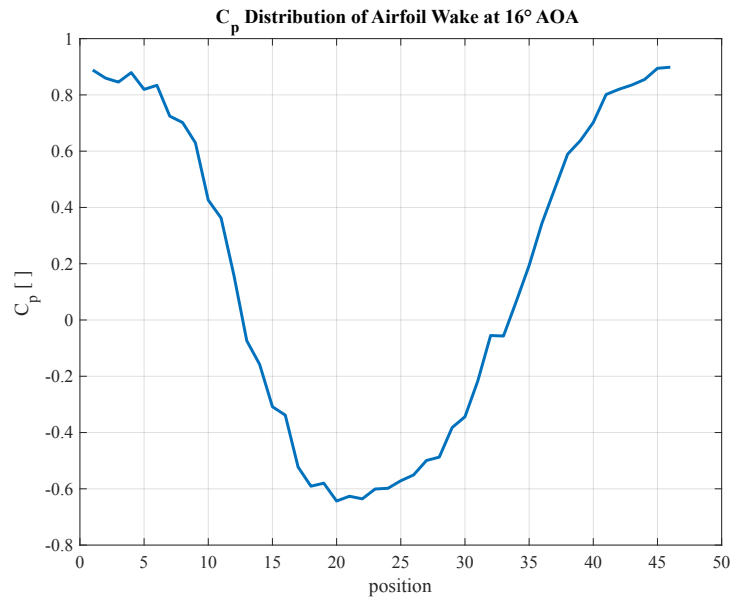


Figure A.8: Plot of C_p distribution vs the Airfoils wake at an AoA of 16°

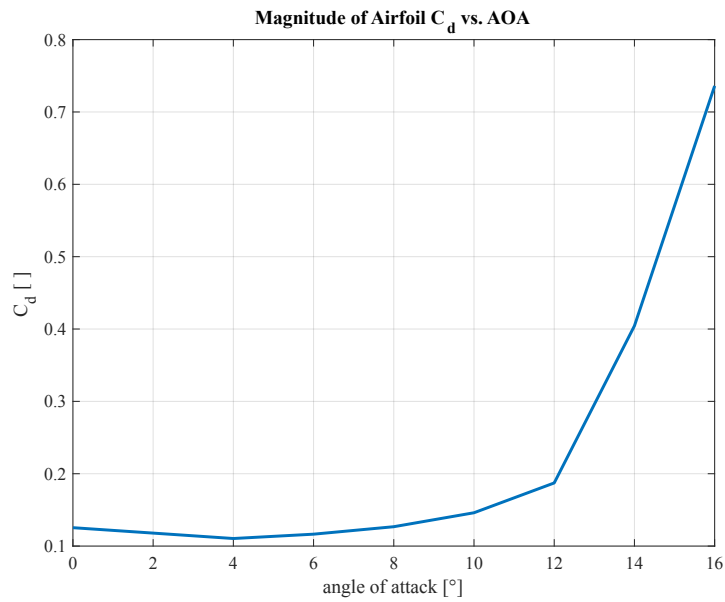


Figure A.9: Plot of the magnitude of the airfoil's C_d vs. the airfoil's AoA.

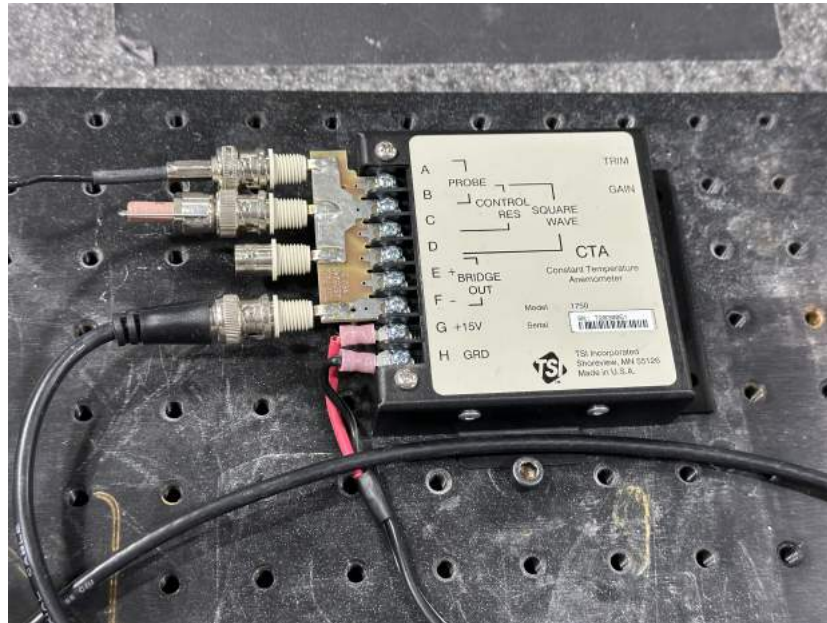


Figure A.10: Image of the Hot Wire data collection computer.

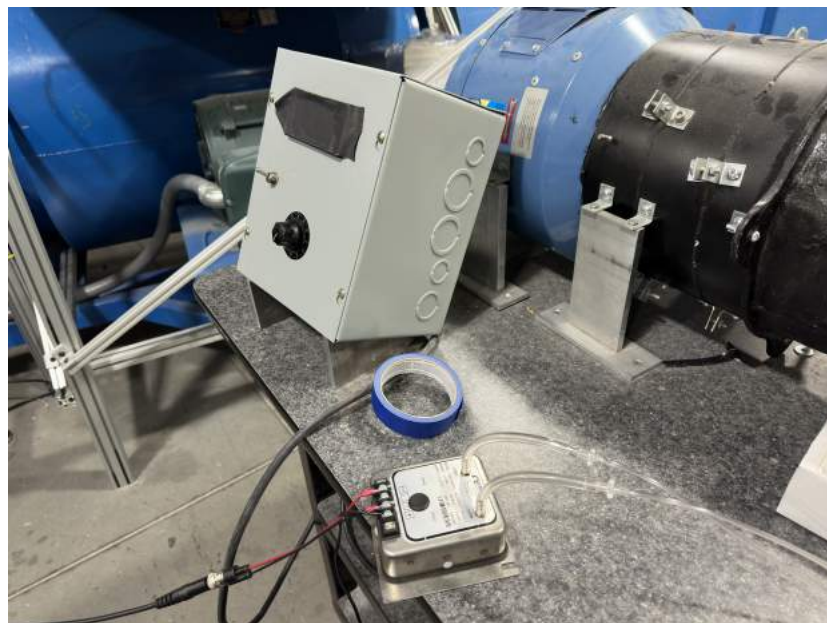


Figure A.11: Open loop wind tunnel speed controller and the Mensor manometer

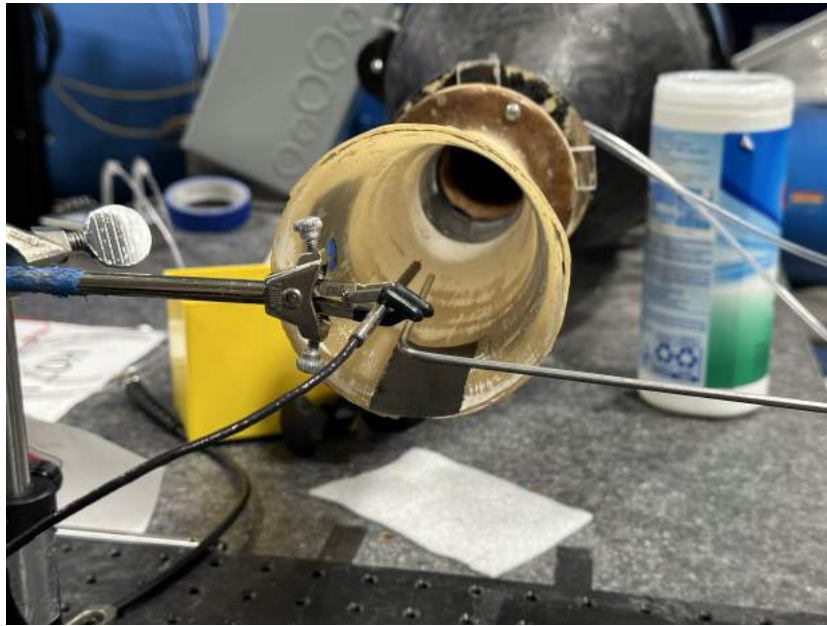


Figure A.12: *Image of the Hot Wire Anemometer inside of open Circuit wind tunnel.*

APPENDIX B

B.1 Data

Table B.1: Coefficient of Pressure, C_p , at taps 1-23 on the pressure rake at different angles of attack.

Tap	0°	4°	6°	8°	10°	12°	14°	16°
1	0.907	0.905	0.905	0.901	0.904	0.902	0.895	0.888
2	0.888	0.880	0.879	0.873	0.878	0.878	0.871	0.860
3	0.883	0.877	0.877	0.872	0.876	0.875	0.863	0.846
4	0.913	0.908	0.908	0.904	0.908	0.907	0.898	0.879
5	0.869	0.847	0.845	0.837	0.848	0.853	0.853	0.819
6	0.922	0.921	0.922	0.920	0.922	0.920	0.886	0.834
7	0.864	0.855	0.856	0.846	0.857	0.851	0.802	0.724
8	0.907	0.907	0.908	0.903	0.907	0.899	0.815	0.702
9	0.910	0.907	0.908	0.903	0.908	0.893	0.788	0.629
10	0.863	0.860	0.861	0.854	0.861	0.822	0.643	0.426
11	0.892	0.889	0.890	0.883	0.880	0.803	0.611	0.362
12	0.911	0.905	0.906	0.893	0.859	0.721	0.480	0.159
13	0.897	0.895	0.890	0.848	0.779	0.597	0.292	-0.074
14	0.897	0.869	0.842	0.753	0.665	0.508	0.208	-0.158
15	0.910	0.836	0.780	0.676	0.586	0.423	0.084	-0.308
16	0.907	0.780	0.690	0.584	0.493	0.352	0.028	-0.338
17	0.879	0.631	0.537	0.459	0.374	0.247	-0.166	-0.523
18	0.881	0.624	0.541	0.498	0.374	0.213	-0.262	-0.591
19	0.793	0.661	0.630	0.611	0.440	0.209	-0.285	-0.580
20	0.724	0.794	0.794	0.785	0.567	0.247	-0.393	-0.643
21	0.633	0.835	0.844	0.836	0.664	0.302	-0.386	-0.626
22	0.593	0.910	0.911	0.907	0.814	0.449	-0.427	-0.636
23	0.531	0.848	0.850	0.843	0.794	0.502	-0.417	-0.601

Table B.2: *Coefficient of Pressure, C_P , at taps 24-46 on the pressure rake at different angles of attack.*

Tap	0°	4°	6°	8°	10°	12°	14°	16°
24	0.597	0.909	0.910	0.908	0.888	0.654	-0.423	-0.598
25	0.632	0.897	0.898	0.894	0.884	0.726	-0.413	-0.571
26	0.702	0.907	0.907	0.905	0.901	0.803	-0.401	-0.551
27	0.731	0.847	0.844	0.839	0.829	0.786	-0.368	-0.499
28	0.837	0.904	0.904	0.901	0.897	0.875	-0.368	-0.487
29	0.878	0.915	0.915	0.913	0.910	0.897	-0.284	-0.382
30	0.864	0.870	0.869	0.864	0.858	0.854	-0.263	-0.344
31	0.913	0.914	0.914	0.912	0.910	0.908	-0.164	-0.217
32	0.899	0.899	0.899	0.897	0.895	0.895	-0.039	-0.055
33	0.909	0.903	0.902	0.899	0.897	0.896	-0.048	-0.057
34	0.891	0.888	0.887	0.883	0.879	0.880	0.046	0.066
35	0.903	0.894	0.891	0.886	0.882	0.881	0.157	0.194
36	0.915	0.911	0.910	0.907	0.904	0.903	0.294	0.344
37	0.888	0.885	0.884	0.880	0.876	0.876	0.404	0.467
38	0.924	0.922	0.921	0.919	0.918	0.917	0.537	0.589
39	0.897	0.890	0.889	0.885	0.882	0.881	0.575	0.638
40	0.909	0.901	0.899	0.896	0.894	0.892	0.654	0.702
41	0.908	0.907	0.907	0.905	0.904	0.904	0.749	0.801
42	0.922	0.918	0.917	0.916	0.915	0.914	0.785	0.820
43	0.898	0.897	0.896	0.894	0.893	0.893	0.794	0.835
44	0.902	0.899	0.898	0.895	0.893	0.893	0.824	0.855
45	0.919	0.918	0.917	0.916	0.915	0.915	0.873	0.895
46	0.914	0.914	0.914	0.912	0.911	0.911	0.878	0.898

Table B.3: *C_d at different airfoil angles of attack.*

	0°	4°	6°	8°	10°	12°	14°	16°
C_d	0.125	0.110	0.116	0.127	0.146	0.187	0.309	0.297

Table B.4: *Manometer pressure, anemometer voltage, and flow velocity values at different percents of wind tunnel motor maximum frequency.*

Percent of Max Freq.	Pressure [in H_2O]	Voltage [V]	Velocity [m/s]
20%	3.005	1.050	10.605
24%	3.028	1.072	11.057
28%	3.048	1.092	11.432
32%	3.078	1.134	11.966
36%	3.106	1.163	12.438
40%	3.154	1.217	13.211
44%	3.193	1.256	13.815
48%	3.246	1.249	14.598
52%	3.315	1.263	15.542
56%	3.388	1.268	16.501
60%	3.461	1.310	17.388

APPENDIX C

C.1 Lab6Analysis.m

```

1  clear; clc; close all;
2
3  %% Knowns
4  figure_dir = "../Figures/";
5  data_dir = "./Data/";
6  % Viscosity calculated at 21.2°C
7  % https://www.engineeringtoolbox.com/air-absolute-kinematic-viscosity-d\_601
8  % .html
9  mu_air = 18.18e-6; % [Pa*s]
10 rho_air = 1.225; % [kg/m^3]
11 V_inf = 19.4; % [m/s] V
12 K = 1.1; % Calibration Constant
13 chord = 0.101; % [m] Chord of airfoil
14 d_taps = 0.002; % [m] Distance between taps
15
16 %% Part 1 Airfoil Wake
17 aoa = [0 4 6 8 10 12 14 16];
18 n_aoa = length(aoa);
19 wake_files = dir(data_dir + '*deg.csv');
20 % Columns containing pressure values from raw data
21 range = cat(2, (2:17), (35: 50), (68: 81));
22 n_taps = length(range); % number of taps
23 position = (1:n_taps); % position of taps
24 PA_idx = 82;
25 PE_idx = 83;
26 C_p = zeros(n_aoa, n_taps); % Initialize matrix for pressure data
27 U_p = zeros(n_aoa, n_taps); % Initialize matrix for velocity data
28 C_D = zeros(1, n_aoa);
29 U_inf = zeros(1, n_aoa);
30 for a = 1:n_aoa % Iterate through files
31     % Read file & find average of columns
32     temp = mean(readmatrix(data_dir+wake_files(a).name));
33     count = 1;
34     PA = temp(PA_idx);

```

```
35     PE = temp(PE_idx);
36     q = K *(PA - PE); % Dynamic Pressure
37     U_inf(a) = sqrt(2 * q / rho_air ); % Freestream velocity
38     for i = 1 : width(temp) % Iterate through data
39         if ismember(i,range) % Take columns with pressure data
40             % Velocity at each tap
41             U_p(a,count) = sqrt(abs((temp(i) - PE)) * 2 / rho_air);
42             if temp(i) - PE < 0
43                 U_p(a, count) = -U_p(a, count);
44             end
45             C_p(a, count) = (temp(i)-PE) / q ; % Cp at each tap
46             count = count + 1;
47         end
48     end
49     % C_P Graphs
50     figure;
51     plot(position, C_p(a,:), "LineWidth", 2);
52     fontname("Times New Roman");
53     fontsize(12, "points");
54     title_str = "C_p Distribution of Airfoil Wake at " + aoa(a) + "° AOA";
55     title(title_str);
56     xlabel("position");
57     ylabel("C_p [ ]");
58     grid on;
59     saveas(gcf, figure_dir + title_str + ".svg");
60
61     % midpoint rule for approx integral
62     for i = 1:n_taps-1
63         f1 = U_p(a, i)/U_inf(a) * (1 - U_p(a, i)/U_inf(a));
64         f2 = U_p(a, i+1)/U_inf(a) * (1 - U_p(a, i+1)/U_inf(a));
65         C_D(a) = C_D(a) + d_taps*((f1 + f2)/2);
66     end
67     C_D(a) = C_D(a) * 2 / chord;
68 end
69
70 figure;
71 hold on;
72 for a = 1:n_aoa % Iterate through files
73     plot(position, C_p(a,:), "LineWidth", 1.5);
74 end
75 hold off;
76 fontname("Times New Roman");
77 fontsize(12, "points");
78 title_str = "C_p Distribution of Airfoil Wake";
79 title(title_str);
80 xlabel("position");
81 ylabel("C_p [ ]");
82 legend("C_p at AOA " + aoa + "°", "Location", "southeast");
83 grid on;
84 saveas(gcf, figure_dir + title_str + ".svg");
85
```

```
86 % C_D Graph
87 figure;
88 plot(aoa, C_D, "LineWidth", 2);
89 fontname("Times New Roman");
90 fontsize(12, "points");
91 title_str = "Airfoil C_d vs. AOA";
92 title(title_str);
93 xlabel("angle of attack [°]");
94 ylabel("C_d [ ]");
95 grid on;
96 saveas(gcf, figure_dir + title_str + ".svg");
97
98 figure;
99 plot(aoa, abs(C_D), "LineWidth", 2);
100 fontname("Times New Roman");
101 fontsize(12, "points");
102 title_str = "Magnitude of Airfoil C_d vs. AOA";
103 title(title_str);
104 xlabel("angle of attack [°]");
105 ylabel("C_d [ ]");
106 grid on;
107 saveas(gcf, figure_dir + title_str + ".svg");
```

C.2 Lab6HotWire.m

```
1 % AER E 344 Spring 2024 Lab 06 Part 2 Analysis
2 % Section 3 Group 3
3
4 clear, clc, close all;
5 figure_dir = "../Figures/";
6 % Initialize arrays
7 pitotTube_inH2O = [];
8 hotWireV = [];
9
10 % Loop through files
11 for fileIndex = 20:4:60
12     % Generate filename
13     filename = sprintf('Data/%d.txt', fileIndex);
14
15     % Read the file
16     data = readtable(filename, 'HeaderLines', 5, 'Delimiter', '\t', 'Format',
17         ↪ '%s%f%f', 'ReadVariableNames', false);
18
19     % Extract columns 3 and 4 from the data table
20     column3 = data.Var2;
21     column4 = data.Var3;
22
23     % Calculate mean values and append to arrays
```

```
23     meanColumn3 = mean(column3);
24     meanColumn4 = mean(column4);
25     pitotTube_inH2O = [pitotTube_inH2O, meanColumn4];
26     hotWireV = [hotWireV, meanColumn3];
27
28
29 end
30
31 % Display pitotTube_inH2O and hotWireV arrays
32 disp('Mean Values for Pitot Tube Pressure [inH2O]:');
33 disp(pitotTube_inH2O);
34 disp('Mean Values for Hot Wire Voltage [V]:');
35 disp(hotWireV);
36
37 % Variables
38 rho_air = 1.195; % [kg / m^3]
39
40 %Estimating the pitot tube V when the motor is off
41 motorFreqPercentage = 0.2:0.04:0.6; % % of max motor frequency
42 P1 = polyfit(motorFreqPercentage, pitotTube_inH2O, 1);
43 pitotTube_inH2Oat0 = P1(2); % pitot tube V when the motor is turned off
44
45 %Calculate v_pt
46 q_pt = (pitotTube_inH2O - pitotTube_inH2Oat0) .* 248.84; % [Pa]
47 v_pt = sqrt(2 .* q_pt ./ rho_air); % [m/s]
48
49 %Display v_T array
50 disp('Flow velocity [m/s]:')
51 disp(v_pt)
52
53 %Calculate and display curve fitting
54 P3 = polyfit(hotWireV, v_pt, 4);
55 x = hotWireV(1):0.01:hotWireV(11);
56 curveFit = P3(1) * x.^4 + P3(2) * x.^3 + P3(3) * x.^2 + P3(4) * x + P3(5);
57 fprintf('4th order polynomial curve fitting formula: \n    %.4fx^4 + %.4fx^3 + %.4fx^2
58     ↪ + %.4fx + %.4f \n\n', P3(1), P3(2), P3(3), P3(4), P3(5))
59
60 %Plot Hot Wire Voltage vs. Air speed
61 scatter(hotWireV, v_pt, 64, "filled");
62 hold on
63 plot(x, curveFit, "LineWidth", 2);
64 fontname("Times New Roman");
65 fontsize(12, "points");
66 title_str = "Velocity vs. Voltage";
67 title(title_str);
68 xlabel('hot wire voltage [V]')
69 ylabel('air speed [m/s]')
70 legend('Experimental data', '4th order polynomial curve fitting', 'Location',
71     ↪ 'SouthEast')
72 grid
73 saveas(gcf, figure_dir + title_str + ".svg");
```
